

Development of a high-sensitivity 80 L radon detector for purified gases

K. Hosokawa¹, A. Murata¹, Y. Nakano², Y. Onishi¹, H. Sekiya^{2,3}, Y. Takeuchi^{1,3,*},
and S. Tasaka⁴

¹*Department of Physics, Kobe University, Kobe, Hyogo 657-8501, Japan*

²*Kamioka Observatory, Institute for Cosmic Ray Research, The University of Tokyo, Higashi-Mozumi, Kamioka, Gifu, 506-1205, Japan*

³*Kavli Institute for the Physics and Mathematics of the Universe, Todai Institutes for Advanced Study, The University of Tokyo, Kashiwa, Japan 277-8583 (Kavli IPMU, WPI)*

⁴*Information and Multimedia Center, Gifu University, Gifu 501-1193, Japan*

*E-mail: takeuchi@phys.sci.kobe-u.ac.jp

Received January 16, 2015; Revised January 23, 2015; Accepted January 23, 2015; Published March 5, 2015

.....
In underground particle physics experiments, the radioactive noble gas ²²²Rn generated from the decay chain of the uranium series could be a serious background source. We have been developing high-sensitivity radon detectors to assay radon in the Kamioka underground laboratory. In order to achieve a further low background level, we developed a new radon detector with better hermeticity. The high-voltage dependence and humidity dependence of the detection efficiencies were obtained through our calibration systems. The background level of the new radon detector was also measured.
.....

Subject Index H20

1. Introduction

The noble gas ²²²Rn is continuously generated from the decay chain of the ²³⁸U series. It has a half-life of 3.82 days and potentially dissolves into water, xenon, argon, and so on. It can be a serious background source for underground experiments.

For example, in the Super-Kamiokande experimental area in Kamioka mine, the radon concentration is about 3000 and 50 Bq/m³ in summer and winter, respectively, because of the wind direction [1]. Thus, if one conducts a direct dark-matter detection experiment by searching for the annual modulation signal [2,3], the radon concentration around the detectors is required to be controlled and kept low.

A higher-sensitivity radon assay would be one of the essential techniques to improve the sensitivity of the underground experiments. Therefore, we have developed a new high-sensitivity radon detector for purified gases, such as xenon, argon, and air.

2. High-sensitivity radon detector for purified gases

We developed a high-sensitivity radon detector (70 L radon detector) [4] for underground experiments in Kamioka. The principle techniques in radon detection are the electrostatic collection of the daughter nuclei of ²²²Rn and the energy measurement of their alpha decays with a PIN photodiode. More than 90% of ²¹⁸Po atoms tend to become positively charged [5]. They will be collected on

the surface of the PIN photodiode by the electric field and alpha decays in the decay chain will be observed.

In order to lower the background level of the 70 L radon detector and measure the radon concentration in purified gases like the noble gas xenon, we have developed a new radon detector (80 L radon detector) [6]. In the 80 L radon detector, knife-edge flanges with metal gasket were used instead of the acrylic plate and Viton O-rings that were used in the 70 L radon detector.

Due to the structure, the lowest vacuum level of the 70 L detector was 10 kPa. After replacing the parts (acrylic plate and O-rings), the vacuum level limit of the 80 L radon detector became less than 10^{-4} Pa.

The detector geometry has also been modified from the 70 L radon detector to apply the same “Grade MC” electrochemical buffing used in another previous radon detector [7]. The volume of the detector vessel increased from 70 L to 80 L. The standard value of the supplied high voltage for electrostatic collection was also changed in the 80 L radon detector.

These development works were done collaboratively among Kamioka Observatory, Gifu University, and Kobe University.

3. Performance of the 80 L radon detector

In order to use the 80 L radon detector in underground particle physics experiments, several basic performance elements were measured with calibration systems that were prepared in Kobe University and in Kamioka Observatory.

3.1. Calibration system

Figure 1 shows a schematic diagram and a picture of the calibration system for the 80 L radon detector in Kobe. The calibration system in Kobe consists of a refrigerator to control absolute humidity, a circulation pump, a dew point meter, a mass flow controller, a ^{222}Rn source, and an 80 L radon detector. A PYLON RNC ^{226}Ra with 78.3 Bq radioactivity was used as the ^{222}Rn source. The accuracy of the radioactivity of the radon source is $\pm 4\%$ according to specification of the device.

The calibration system in Kamioka consists of almost the same devices, but an ionization chamber was also used as an alternative device to estimate the radon concentration in the system. We assigned $\pm 5\%$ uncertainty as the accuracy of the ionization chamber from the variation of the output values under the same measurement conditions. The details of the calibration system in Kamioka will be explained in a future publication (Y. Nakano et al., manuscript in preparation).

A different 80 L radon detector from that in Kobe was used in Kamioka. We carried out several measurements in both Kobe and Kamioka, then compared the results. We assigned $\pm 10\%$ uncertainty as the systematic difference between the different 80 L detectors. Within this uncertainty, the results from both sites were consistent.

3.2. Energy spectrum

Figure 2 shows a typical pulse height distribution from alpha decays of ^{222}Rn daughter nuclei. Since ^{214}Po exists at a lower stream of the decay chain, the radon detector has a higher collection efficiency for ^{214}Po than ^{218}Po . Furthermore, alpha-rays emitted from ^{212}Bi decay in a Th-series decay chain could overlap with the ^{218}Po signal region. Thus, the ^{214}Po peak was used to measure ^{222}Rn concentration. For example, in this measurement, the analog-to-digital converter (ADC) channels from 169 to 179 contain 90% of signals in the ^{214}Po peak and were selected as the ^{214}Po signal region to obtain the integrated count rate in count/day. The supplied voltage value and the settings of the amplifier

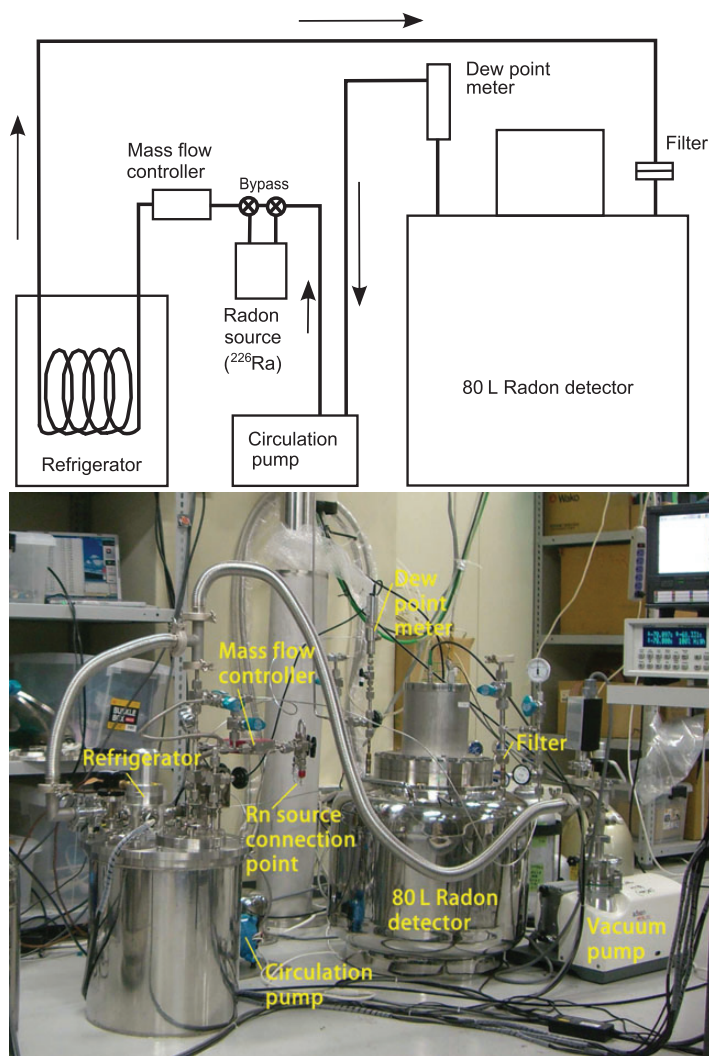


Fig. 1. Schematic diagram of the 80 L radon detector calibration system in Kobe. A picture of the system is also shown.

affect the peak position. In each measurement condition, this pulse height distribution was checked, then the appropriate ADC region was used for the integration window.

3.3. Calibration factor

The calibration factor (CF) in (count/day)/(mBq/m³) was used to obtain the radon concentration in mBq/m³ from the integrated ²¹⁴Po count rate in count/day. Using the calibration system, the dependence of the calibration factor on the supplied high-voltage value and/or humidity of the purified gases was obtained.

3.3.1. High-voltage dependence

Reverse bias minus high voltage was supplied to the PIN photodiode of the 80 L radon detector. An electric field between the photodiode and stainless steel vessel was formed by the supplied high voltage. The high-voltage value affects the electrostatic collection efficiency of the ²²²Rn daughter nuclei. Thus, the calibration factor depends on the supplied high-voltage value.

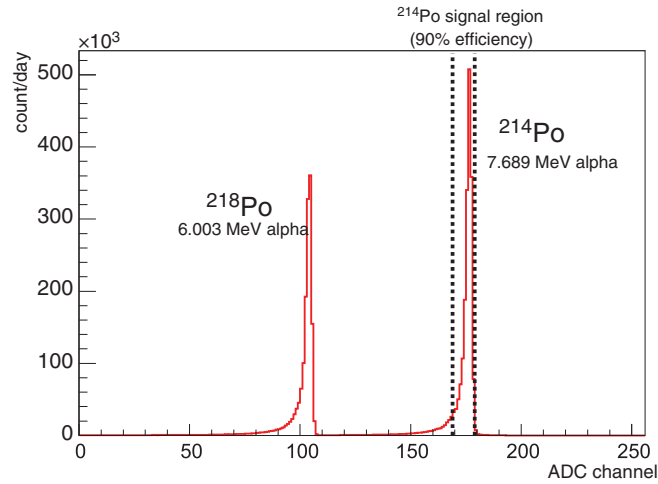


Fig. 2. Typical pulse height spectrum of ^{222}Rn daughter signals.

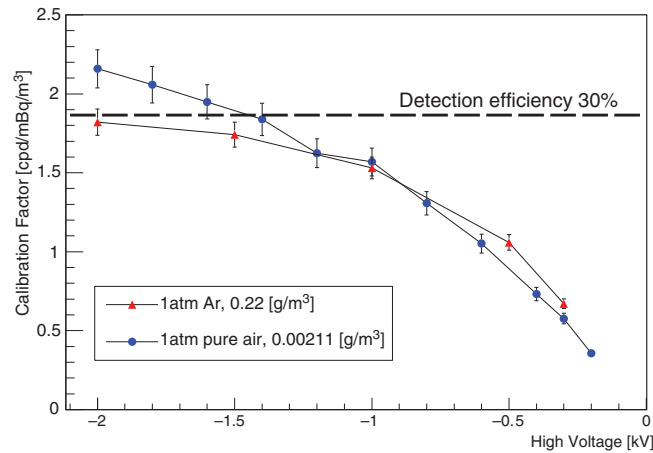


Fig. 3. The calibration factor of 80 L radon detectors as a function of supplied high-voltage value. The Ar and air data were taken with the calibration systems in Kobe and in Kamioka, respectively. The error bar shows systematic uncertainties of the measurements. Here, the uncertainties of the dew point measurement and the radon concentration are included. See text for details on the dashed line.

The high-voltage dependences of the calibration factors were measured with the calibration systems in both Kobe and Kamioka. The result is shown in Fig. 3. The calibration data were taken with the Rn source and G2-grade Ar gas (>99.9995 vol.%) or G1-grade air (impurity <0.1 vol. ppm) at atmospheric pressure. The averaged absolute humidities for Ar and air were 0.22 g/m^3 and 0.0021 g/m^3 , respectively. The supplied high-voltage values were changed from -0.2 kV to -2.0 kV . The calibration factor rises with higher supplied voltage value, as expected. The dashed line shows 30% detection efficiency of the 80 L radon detector for ^{214}Po , assuming 90% efficiency of the ADC integration region. Note that the maximum detection efficiency would be 50% considering the direction of the alpha decays on the photodiode surface. This means that 60% of the radon daughter nuclei were collected by the electrostatic field at the 30% detection efficiency line. The same line is also drawn in Fig. 5.

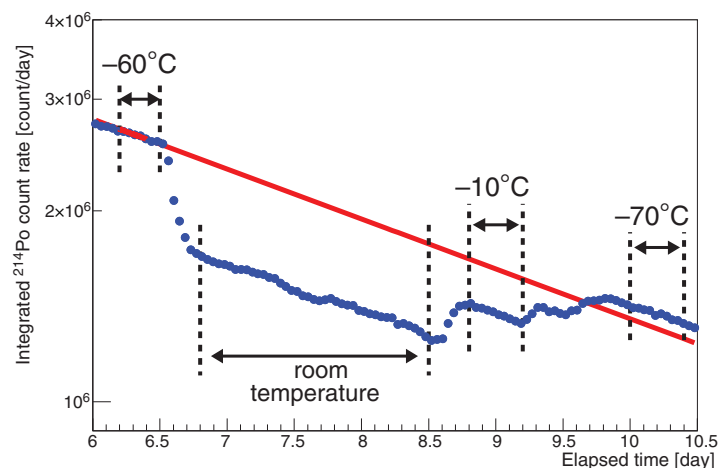


Fig. 4. An example of the variation of the integrated count rate of ^{214}Po in the 80 L radon detector with different dew point values. The solid red line shows a fit to the data at -60°C with the expected radon decay constant. The vertical dashed lines indicate the regions used to obtain the CF.

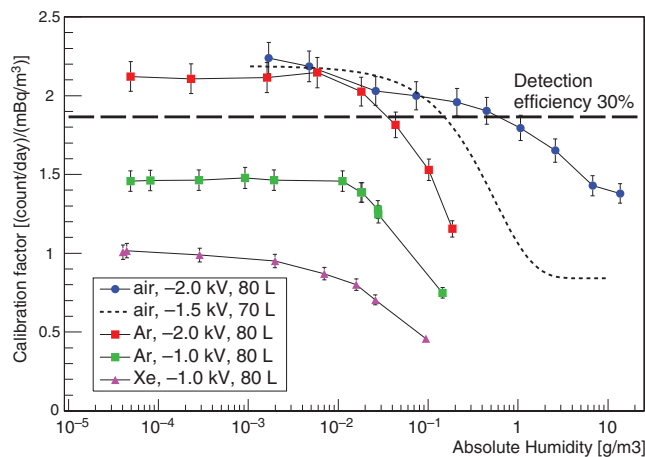


Fig. 5. The calibration factor of the 80 L radon detector as a function of absolute humidity. The dotted line shows that of the 70 L radon detector [4]. The air data were taken in Kamioka, and others were taken in Kobe. For details on the dashed line and the error bars, see Fig. 3.

We choose -2.0 kV as the standard high-voltage value for Ar and air. For Xe, we choose -1.0 kV as the standard value, since a discharge around the feed-through of the PIN photodiode was observed in some calibration runs at -2.0 kV .

3.3.2. Humidity dependence

Concerning the electrostatic collection method, the neutralization effect of ^{218}Po atoms is known [8]. Therefore, humidity dependence calibrations were conducted.

Using a refrigerator, we controlled the dew point temperature, i.e., the absolute humidity. Figure 4 shows an example of the calibration run. In this measurement, the radon source was bypassed from the calibration system after supplying radon gas to the system. Therefore, both the radon decay and the dependence of the integrated ^{214}Po count can be seen in the plot.

The calibration factor as a function of absolute humidity is shown in Fig. 5. The black dotted line shows the calibration factor of the 70 L radon detector. Colored plots show the calibration factor of

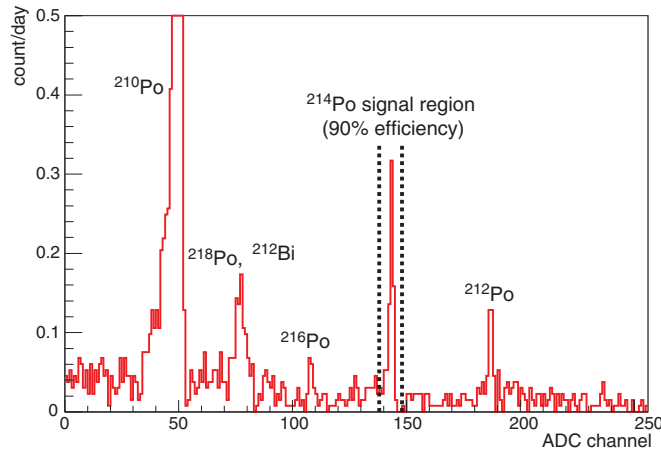


Fig. 6. Pulse height spectrum in the background run with purified air under 1 atmospheric pressure and -2.0 kV high-voltage value in Kobe. ADC channel 137–147 was used as the ^{214}Po signal region. The huge peak at around 50 ADC count is due to ^{210}Po , which was accumulated during the calibration measurements.

the 80 L radon detector. G1-grade air, special-grade Ar (99.999%), and purified Xe were used for these measurements. The air data were taken in Kamioka, and others were taken in Kobe.

We estimated the total systematic uncertainties in these calibration factor measurements as 12%. The sources of the systematic uncertainties were the following: difference in the 80 L detectors 10%, accuracy of the radon concentration 5%, accuracy of the dew point meter 2%, and accuracy of the total volume estimation of the calibration system 2%. Regarding the accuracy of the radon concentration, we took the larger uncertainties from the ionization chamber.

Therefore, the obtained calibration factor of the 80 L radon detector became as follows:

- 2.2 ± 0.3 (stat. + syst.) (count/day)/(mBq/m³) (at 0.002 g/m³, -2.0 kV, air)
- 2.1 ± 0.2 (stat. + syst.) (count/day)/(mBq/m³) (at 0.002 g/m³, -2.0 kV, Ar)
- 0.95 ± 0.11 (stat. + syst.) (count/day)/(mBq/m³) (at 0.002 g/m³, -1.0 kV, Xe).

3.4. Background level

Figure 6 shows the pulse height spectrum of 132.5 days' live-time background data in Kobe. After evacuating the 80 L radon detector, purified air was filled to atmospheric pressure level, then the inlet and outlet valves were closed. The supplied high-voltage value was -2.0 kV in this background run.

The integrated count in the ^{214}Po signal region during the background run was 107 count. Therefore, the obtained background level of the 80 L radon detector was 0.81 ± 0.08 (stat. only) count/day.

The background level of the 70 L radon detector for air was 2.4 ± 1.3 count/day [4]. The background level of the 80 L radon detector has been lowered by a factor of 3 from the 70 L radon detector.

In Fig. 6, some noise hits were observed during the background run, at around ~ 0.02 count/day/bin level. However, if we just apply the calibration factor for purified air, the corresponding radon concentration during the background run becomes 0.37 ± 0.05 (stat. only) mBq/m³.

4. Conclusion

A new high-sensitivity radon detector (80 L radon detector) has been developed. The basic performances of the 80 L radon detector have been studied.

From the high-voltage dependence of the 80 L radon detector, we chose -2.0 kV as the standard voltage to supply for the measurements with purified air and argon. For purified xenon, we chose -1.0 kV as the standard voltage.

As the calibration factor of the 80 L radon detector, we obtained the following values at 0.002 g/m³ absolute humidity and standard high-voltage conditions: Air: 2.2 ± 0.3 (stat. + syst.) (count/day)/(mBq/m³), Ar: 2.1 ± 0.2 (stat. + syst.) (count/day)/(mBq/m³), and Xe: 0.95 ± 0.11 (stat. + syst.) (count/day)/(mBq/m³). The calibration factor for air is comparable with our previous 70 L radon detector. The calibration factors for Ar and Xe were newly obtained in this work.

As the background level of the 80 L radon detector, we obtained 0.81 ± 0.08 (stat. only) count/day with purified air and -2.0 kV high-voltage value. This count rate is about one-third of the 70 L radon detector's background level. Owing to the improved hermeticity of the 80 L radon detector and the improved electropolishing, the background level was lowered.

The background level of the 80 L radon detector corresponds to a 0.37 ± 0.05 (stat. only) mBq/m³ radon concentration. This provides a high-sensitivity radon assay in μ Bq/m³ concentration in the application of this 80 L radon detector in underground particle physics experiments.

Acknowledgements

This work was supported by JSPS KAKENHI Grant-Number 24340050, 25.2848, and ICRR Joint-Usage.

References

- [1] S. Fukuda et al., Nucl. Instrum. Meth. A, **501**, 418 (2003).
- [2] K. A. Drukier et al., Phys. Rev. D, **33**, 3495 (1986).
- [3] K. Freese et al., Phys. Rev. D, **37**, 3388 (1988).
- [4] Y. Takeuchi et al., Nucl. Instrum. Meth. A, **421**, 334 (1999).
- [5] P. Kotrappa et al., Health Phys., **46**, 35 (1981).
- [6] K. Hosokawa et al., J. Phys.: Conf. Ser., **469**, 012007 (2013).
- [7] C. Mitsuda et al., Nucl. Instrum. Meth. A, **497**, 414 (2003).
- [8] T. Iida et al., Health Phys., **54**, 139 (1988).